Eur Biophys J (2009) 38:437–446
DOI 10.1007/s00249-008-0389-6

ORIGINAL PAPER

Thermal aggregation and ion-induced cold-gelation of bovine serum albumin

Giovanna Navarra · Daniela Giacomazza · Maurizio Leone · Fabio Librizzi · Valeria Militello · Pier Luigi San Biagio

Received: 16 July 2008 / Revised: 5 December 2008 / Accepted: 7 December 2008 / Published online: 9 January 2009

Abstract Protein cold-gelation has recently received particular attention for its relevance in bio and food technology. In this work, we report a study on bovine serum albumin cold-gelation induced by copper or zinc ions. Metal-induced cold-gelation of proteins requires two steps: during the first one, the heat treatment causes protein partial unfolding and aggregation; then, after cooling the solution to room temperature, gels are formed upon the addition of metal ions. The thermally induced behaviour has been mainly investigated through different techniques: Fourier transform infrared (FTIR) spectroscopy, circular dichroism, dynamic light scattering (DLS) and rheology. Data have shown that the aggregation process is mainly due to protein conformational changes—α-helices into β-aggregates—forming small aggregated structures with a mean diameter of about 20 nm a few minutes after heating. After metal ion addition, the viscoelastic properties of the gels have been investigated by rheological measurements. The behaviour of the elastic and viscous moduli as a function of time is discussed in terms of ion concentration and type. Our results show that: (1) the elastic behaviour depends on ion concentration and (2) at a given ion concentration, gels obtained in the presence of zinc exhibit an elastic value larger than that observed in the Cu^{2+} case. Data suggest that cold-gelation is the result of different mechanisms: the ion-mediated protein–protein interaction and the bridging effect due to the presence of divalent ions in solution.

Keywords Bovine serum albumin (BSA) · Proteins aggregation · Metal ions · Cold-gelation

G. Navarra · D. Giacomazza (✉) · M. Leone · V. Militello · P. L. San Biagio
Consiglio Nazionale delle Ricerche, Istituto di Biofisica, U. O. di Palermo, Via U. La Malfa 153, 90146 Palermo, Italy
e-mail: daniela.giacomazza@pa.ibf.cnr.it

G. Navarra · M. Leone · F. Librizzi · V. Militello
Dipartimento di Scienze Fisiche ed Astronomiche, Università di Palermo, Via Archirafi 36, Palermo, 90123 Palermo, Italy

Introduction

Gelation of globular proteins is a very interesting subject because of its physical and industrial implications (Mulvihill and Kinsella 1987; Ziegler and Foegeding 1990; Bryant and McClements 1998; Allain et al. 1999; Le Bon et al. 1999; Lefevre and Subirade 1999; Gosal and Ross-Murphy 2000; Gosal et al. 2004a, b). It is well known that, under appropriate conditions, native proteins can undergo conformational changes leading to aggregation and, above a critical protein concentration, to gelation (Dobson 2004; Doi 1993).

Many parameters affect directly or indirectly the gelation rate and the final "gel strength", such as amino acid sequence, protein concentration, pH and ionic strength (Gosal and Ross-Murphy 2000). Recently, research interest has been moving towards cold-gelation of proteins. In fact, this alternative way to obtain gels from proteins allows immediate applications in food technology, in biotechnology and, in particular, in tissue engineering because gel formation does not need high temperatures, incompatible with the cell life.

It is generally accepted that the physical and chemical properties of cold-gels depend on the temperature of the heat treatment, the ratio between the concentration of the element inducing cold-gelation and the native protein concentration, and the pH of the solution. In particular, the

temperature of the heat treatment has a significant influence on the rate of gelation and on the morphological aspect of the final gel, while the protein concentration mainly affects the mechanical properties of gels formed (Bryant and McClements 1998).

While it is accepted that a critical protein concentration exists, below which no percolative network is formed, there are different opinions on the existence of a critical temperature. However, it has been observed that the rate of the gelation process decreases while reducing the treatment temperature (Tobitani and Ross-Murphy 1997; Le Bon et al. 1999).

The interactions and the structure of cold gels have been studied after addition of salts to heat-treated solution of proteins (Hongsprabhas and Barbut 1997a, b, c; Hongsprabhas et al. 1999; Bryant and McClements 2000; Marangoni et al. 2000; Alting et al. 2000, 2003a, b, 2004; Remondetto et al. 2002; Remondetto and Subirade 2003). Remondetto et al. (2002) and Remondetto and Subirade 2003 have studied cold-set gels induced by addition of divalent iron ions in solutions of heated β-Lactoglobulin (βLg). Their results have shown that the macroscopic properties of βLg gels, obtained after Fe^{2+} addition, were similar to those obtained in presence of Ca^{2+}, Mg^{2+} and Na^{+} (Barbut and Foegeding 1993; Bryant and McClements 1998; Hongsprabhas and Barbut 1997c), suggesting that the electrostatic interactions play a dominant role; moreover, they have also observed that the gel structure, fine stranded or particulate, depends on pH conditions and protein/iron ratio.

Studies on the heat-induced gelation of bovine serum albumin (BSA) at different pH (Boye et al. 1996; Veerman et al. 2003) have shown that the gelation process is affected by some salts. In particular, the texture and the rheological properties of the gels depend on the amount of salts in solution. Some authors have demonstrated that the addition of NaCl in the BSA solution at neutral pH increased the gel strength by decreasing the electrostatic repulsion between proteins and that the simultaneous presence of both sodium and calcium ions further strengthened the BSA gel (Donato et al. 2005). Haque and Aryana (2002) have investigated the effects of very low concentrations of $CuSO_4$, $FeSO_4$, $ZnSO_4$ and $MgSO_4$, on the structure of BSA gels by transmission and scanning electron microscopies. The comparison with pure BSA gel has shown that the addition of $CuSO_4$ markedly changed the microstructure of BSA gels: significantly larger water entrapping void spaces were seen and the gel matrix is comprised larger aggregates. The same authors observed that, in presence of Zn^{2+}, aggregates are more compact and appear less clustered and fused together than in presence of Cu^{2+}.

The present work has the purpose of elucidating the mechanism involved in the gelation of BSA proteins at room temperature in presence of different concentrations of copper (Cu^{2+}) and zinc (Zn^{2+}), for the first time. In the native state, BSA is characterized by three domains, each one formed by six helices, and its secondary structure is essentially α-helical (Gelamo and Tabak 2000; Gelamo et al. 2002). Its isoelectric point is around 5 while at pH = 7 BSA has about 10 effective negative charges per protein molecule (Fogh-Andersen et al. 1993; Carter and Ho 1994; Böhme and Scheler 2007). At room temperature, tertiary structure is well defined and stabilized. As temperature increases, some molecular regions become accessible to new intermolecular interactions, producing pH dependent soluble aggregates through disulphide and non-covalent bonds (Wang 1999; Honda et al. 2000; Militello et al. 2004). Moreover, it has been reported that, in the whole BSA aggregation process, an important role is also played by the liquid–liquid demixing (LLD) due to the thermodynamic instability of the solution (San Biagio et al. 1999). In particular, BSA aggregation appears to be the result of no less than three interconnected mechanisms: critically diverging concentration fluctuations associated with LLD, conformational changes and protein cross-linking (San Biagio et al. 1996, 1999). However, the hierarchy of these mechanisms is strictly dependent on the experimental conditions (Militello et al. 2003).

In the first part of the present work, we describe the effect of heat treatment on the protein, below the denaturation temperature, by dynamic light scattering (DLS) and infrared spectroscopy measurements. This treatment leads to the formation of small aggregates, which are the constituting units of the larger aggregates present in the gel state. Finally, after cooling the sample and addition of different concentrations of Cu^{2+} or Zn^{2+}, we characterize the mechanical properties of the final gels by rheological measurements. We focus on the effects of Cu^{2+} and Zn^{2+} since they may have important medical applications being involved in aetiology and therapy of some illness, such as Menkes and Wilson diseases.

Materials and methods

Sample preparation

Bovine serum albumin was purchased from Sigma-Aldrich. Powdered protein was dissolved in a 20-mM MES solution (4-Morpholineethanesulfonic acid), prepared in H_2O or D_2O (99.9%, Aldrich) and titred with KOH or KOD to obtain pH or pD = 7 (where pD = pH + 0.4). The final concentration of protein was 1 mM (66 mg/ml). The protein solutions were centrifuged (380*g* for 8 min) and filtered with Sartorius filters having a pore diameter of 0.20 μm. The freshly prepared samples in D_2O were divided in two aliquots for IR and scattering measurements,

respectively, in order to characterize the heating phase at 58°C of native protein solution. D_2O solutions were used to avoid the IR spectral overlaps between Amide I band and the strong water absorption band in the region around 1,650 cm^{-1}. The freshly prepared samples in H_2O were incubated at 58°C for 2 h under weak stirring.

$CuCl_2$ or $ZnCl_2$ (99.999%, Sigma-Aldrich) prepared at different concentrations in Super Q Millipore water were added as one tenth of the final solution volume to previously heated BSA solutions after cooling them to room temperature, in order to obtain a final concentration of 1, 5, 8,10, 15, 20 and 30 mM.

IR measurements

IR spectra were measured with a Bruker Vertex 70 spectrophotometer, equipped with a MIR global light source (i.e. U-shaped silicon carbide piece). The spectral resolution is 2 cm^{-1}; each spectrum is obtained averaging over 100 scans. All samples were placed between two CaF_2 windows, with a 0.05 mm Teflon spacer. Each absorption spectrum was corrected for the contribution of the empty beam line and for the residual water vapour spectrum. The error on the wavenumber estimation was ± 0.5 cm^{-1} with absorbance accuracy within 1%. In order to identify the time evolution of each spectral component under the broad amides band, difference spectra were obtained by subtracting from the spectrum at a generic time t_i the spectrum at t_0 (where t_0 was taken 7 min after the beginning of the experiment to reach the thermal equilibrium). Data here reported were made at least in triplicate.

The spectral zones investigated are the Amide I and Amide II regions. Amide II band (1,400–1,580 cm^{-1}) is predominantly associated with the N–H in-plane bending (Bakker et al. 2005) and shifts towards lower wavenumbers when a H–D exchange occurs (Amide II′ band); it reveals the replacement of the hydrogens located in the core of the native protein when a heat-induced partial opening of the protein takes place. Amide I band (1,580–1,720 cm^{-1}) is an infrared absorption band attributed to an out of phase combination of C=O and C–N stretching of amide groups, giving information on the secondary structure and supramolecular arrangement of BSA molecules. In the presence of D_2O, the band shifts towards 1,650 cm^{-1} (Amide I′ band) (Dong et al. 1990). Generally, it has a composite profile consisting of several spectral components related to the different types of secondary structures (Byler and Susi 1986; Dong et al. 1990; Cai and Singh 1999; Pelton and Mec Lean 2000), as summarized in Table 1. The time evolution of the main spectral components of the band during thermal treatment is a probe of protein structural changes in terms of α-helix, random coil and β-sheet content, and it gives information on the intermolecular aggregation (β-aggregates) through the appearance of two shoulders at about 1,620 and 1,680 cm^{-1} (Fang and Dalgleish 1997; Qi et al. 1997; Fink 1998; Allain et al. 1999; Lefevre and Subirade 1999; Militello et al. 2003; Remondetto and Subirade 2003). In particular, the bands due to intermolecular aggregation are at about 1,614 and 1,685 cm^{-1} and are assigned to vibrations of strongly bound intermolecular β-strands and anti-parallel β-sheets, respectively (Allain et al. 1999; Remondetto and Subirade 2003; Navarra et al. 2007). Since the spectral region between 1,630 and 1,650 cm^{-1} is attributed to α-helices, disordered random coils and intramolecular β-sheets (Remondetto and Subirade 2003; Navarra et al. 2007), its decreasing, together with the increase of the intensity at about 1,620 cm^{-1}, is a signature of the conversion from α-helices and intramolecular β-structures into β-aggregates.

Table 1 Spectral position of the Amide I′ band contributions related to the several secondary structures

Structure type	Spectral position (cm^{-1})
β-sheet	1625–1640
	1670–1680
α-helix	1651–1657
β-aggregates	1610–1623
	1675–1695
β-turn	1670–1690
Random coil	1640–1650

DLS measurements

Dynamic light scattering measurements were done using a Zetasizer Nano-S90 (Malvern Instruments) equipped with a He–Ne laser source tuned at 633 nm. Data were collected at 90°. The sample compartment was completely self enclosed and the sample temperature was automatically controlled within 0.1°C. To compare the results with those obtained by IR spectroscopy, intensity scattering data were collected after a thermal equilibration time of 7 min. If necessary, temperature scanning has been done at a rate of 0.2°C/min.

As is well known, DLS gives information on the size of particles in solution. In fact, the intensity autocorrelation function can be written as (Berne and Pecora 1976):

$$g_2(t) = 1 + |g_1(t)|^2 \quad (1)$$

where $g_1(t)$ is the field autocorrelation function. For a monodisperse solution of non-interacting small particles:

$$g_1(t) = Ae^{-DK^2t} \quad (2)$$

where $k = 4\pi n \frac{\sin\frac{\theta}{2}}{\lambda}$ is the scattering vector with n, refraction index of solution; λ, wavelength of the incident light and θ,

the scattering angle (90° in our case). D is the diffusion translational coefficient. For spherical particles, the diameter d can be obtained from:

$$d = \frac{KT}{3\pi\eta D} \tag{3}$$

where K is the Boltzmann's constant, T the temperature and η the solvent viscosity.

Autocorrelation data were preliminarily analyzed using the cumulants method to obtain the mean size (Z-average diameter) of the particles present in solution. More detailed information on the size distribution of the species in solution was obtained by using CONTIN (Provencher 1982).

Circular dichroism (CD) measurements

Circular dichroism measurements were performed on a Jasco J-815 instruments. Measurements were done on BSA native and BSA after 2 h of incubation at $T = 58$°C at the temperature of 20°C. Before CD measurements, the initial BSA concentration (1 mM) was diluted in MES buffer to obtain a final protein concentration of 0.01%. Data have been corrected for the buffer and expressed as mean residue ellipticities, defined as $[\theta] = 100 \times [\theta_{\text{read}}/(l \times c)]$ where θ_{read} is the observed ellipticity in (°), c is the protein concentration in residue mole per litre and l is the cell optical path in cm.

Rheological measurements

Rheological measurements were performed on a stress controlled AR 1000 rheometer (TA Instruments, USA) using a titanium-cone/plate geometry (angle 0.0174 rad, radius 20 mm, gap 26 μm).

Viscoelastic spectra were done on the native protein solution and at the end of the incubation time in the frequency range 0.1–200 rad/s, at a strain of 1×10^{-3}.

Kinetic measurements were obtained from cycles of viscoelastic spectra, with a pause of 1 h, performed in the frequency range 0.1–200 rad/s, at a strain of 1×10^{-3}, well within the linear viscoelastic region. The protein suspension, with the added salt, was gently stirred and placed on the rheometer plate, set at the temperature of 20°C. The thin sample–air interface was coated with silicone oil to avoid water evaporation. All measurements were done in triplicate.

Results and discussion

Heating step characterization

The heating step of cold-gelation carried out on BSA solution has been mainly characterized by DLS and Fourier transform infrared (FTIR) absorption measurements to follow the growth of the particles in solution and the time evolution of changes of secondary and tertiary structures during protein incubation at 58°C for 2 h. CD measurements have been done to observe the protein structural changes occurring after the heating time.

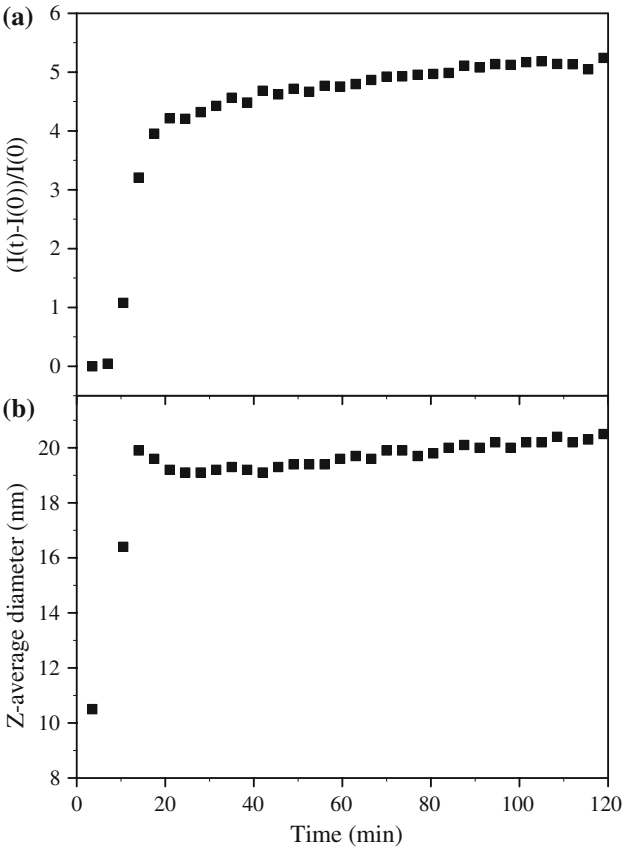

Fig. 1 Time evolution of the normalized scattered intensity (**a**) and of the average diameter (**b**) of BSA (1 mM) at pH = 7 and $T = 58$°C

Figure 1a shows the time evolution of the normalized total scattered intensity of native BSA. As can be noted, within about 20 min BSA molecules undergo an aggregation process inducing the formation of small aggregates with a mean Z-averaged diameter of about 20 nm, whose time evolution is shown in Fig. 1b. Analysis of data, as illustrated in Sect. DLC measurement, has allowed us to obtain the distribution of the diameter values with respect to the particle number in solution and to the scattered intensity at different times.

The size distributions by number (a) and by intensity (b) at initial (t_0), intermediate (t_m) and final experimental (t_f) times are plotted in Fig. 2. As shown in Fig. 2a, through the distribution of the diameter sizes with respect to the particle numbers in solution, we note that after 2 h of incubation at 58°C small aggregates are mainly present, whose dimensions do not change up to 8 h (data not

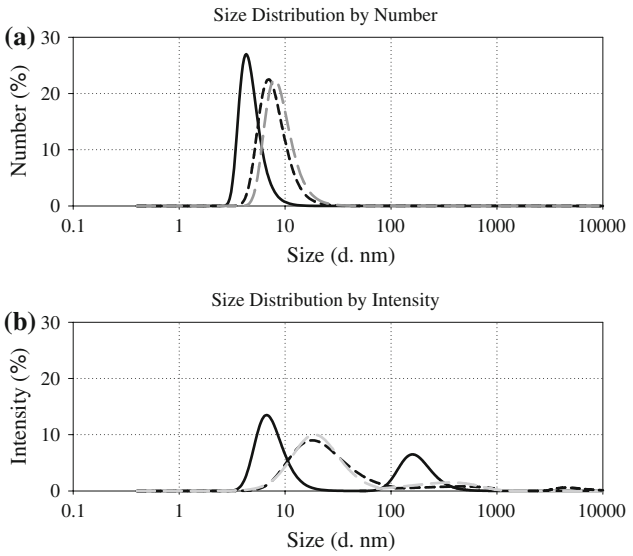

Fig. 2 BSA (1 mM) size distribution of aggregates dimension based: **a** on the numbers of particles present in solution and **b** on the intensity of scattered light at initial ($t_i = 7$ min, *black solid line*), intermediate ($t_m = 20$ min, *black short dashed line*) and final times ($t_f = 120$ min, *gray long dashed line*) of the kinetics at $T = 58$°C

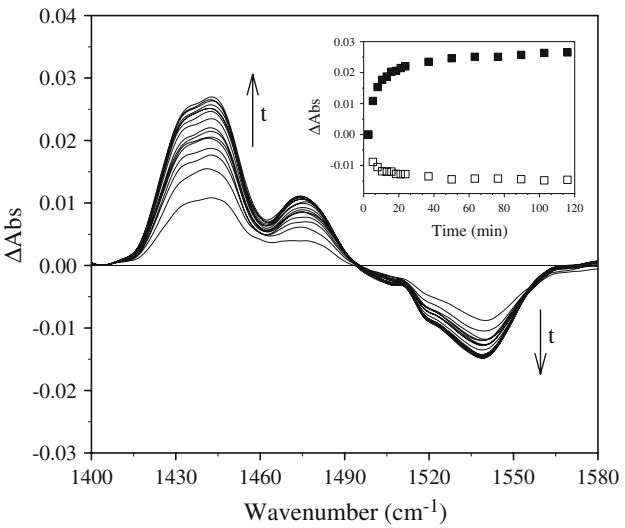

Fig. 3 Infrared absorption difference spectra in the Amide II and Amide II′ region for BSA (1 mM) defined as $\Delta A(t) = A(t) - A(t = 0)$ at pH = 7 and $T = 58$°C. In the inset, the time evolution of the difference absorption intensity of (■) Amide II′ component at 1,442 cm^{-1} and (□) Amide II component at 1,540 cm^{-1} are shown

shown). Furthermore, the observation of the diameter distribution based on the intensity (Fig. 2b) shows that at intermediate and final times two species, characterized by a diameter size of about 20 and 400 nm, are present in solution. Despite its dimension, the larger species is present in a very low concentration as evidenced by comparison of Figs. 2a, b. Finally, at t_0 a species with a large diameter size (several hundred nanometres) is also observed, probably consisting of very few metastable clusters with a short lifetime (Pan et al. 2007). Their formation occurs a few minutes after sample preparation and their intensity remarkably decreases with incubation time at 58°C (Fig. 2b).

Changes of the tertiary and secondary structures of protein in solution have been explored in the IR range. We have first focused our interest on the study of the Amide II band to investigate the time evolution of the tertiary structure; indeed, it reveals the replacement of the hydrogens located in the core of the native protein when a heat-induced partial opening of the protein takes place (see Sect. IR measurements). The IR difference absorption spectra of BSA solutions, at different incubation times, are shown in Fig. 3 in the Amide II and II′ regions. As can be observed, the signal due to Amide II decreases while that of Amide II′ increases as a function of time, indicating the occurrence of partial unfolding of the proteins (Kavanagh et al. 2000). In the inset, the time evolutions of both Amide II ($\sim$1,540 cm^{-1}) and Amide II′ ($\sim$1,450 cm^{-1}) are highlighted; as can be noted, the signals reach a plateau in about 20 min. Comparison of data in Figs. 1 and 3 suggests that, under these experimental conditions, the aggregation of BSA proceeds side by side with a partial unfolding of the protein.

Changes of the BSA secondary structure have been followed through the investigation of the Amide I region. Figure 4a shows the absorption spectra at 58°C of BSA at the initial and final times of the kinetics, suggesting that structural changes have occurred after 2 h of protein incubation. In particular, the absorption intensity at about 1,615 cm^{-1} is increased while the spectral component at about 1,650 cm^{-1} is decreased, indicating that an aggregation process has occurred via conversion of α-helices into intermolecular β-sheets. The difference absorption spectra of the Amide I′ band for BSA protein solution in the IR region between 1,580 and 1,720 cm^{-1} at different incubation times (time increases in the arrows direction) are shown in Fig. 4b. The changes in the difference spectra clearly show the time evolution of each component of Amide I′ and they identify modifications in the secondary structure of BSA. Data show that the components at 1,615 and 1,685 cm^{-1} increase as a function of time, suggesting that aggregation occurs, as confirmed by light scattering measurements, through formation of small aggregates. We underline that the spectral component assigned to β-aggregated sheets has its maximum at 1,615 cm^{-1}, suggesting the existence of stronger H-bonds (Allain et al. 1999; Remondetto and Subirade 2003; Navarra et al. 2007).

Indeed, mechanical spectra (Fig. 5a) carried out at room temperature immediately after the incubation period have shown that the protein solution presents a weak solid-like

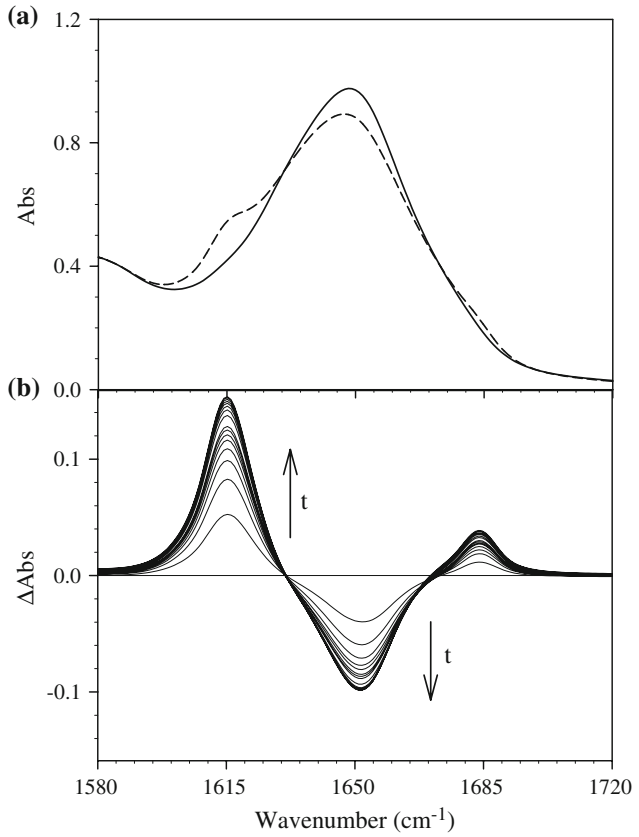

Fig. 4 **a** Absorption spectra in the Amide I′ region for BSA (1 mM) at pH = 7 and at $T = 58$°C at the initial (*solid line*) and final (*dashed line*) incubation times and **b** infrared absorption difference spectra defined as $\Delta A(t) = A(t) - A(t = 0)$ recorded during the incubation time for BSA (1 mM) at pH = 7 and at $T = 58$°C

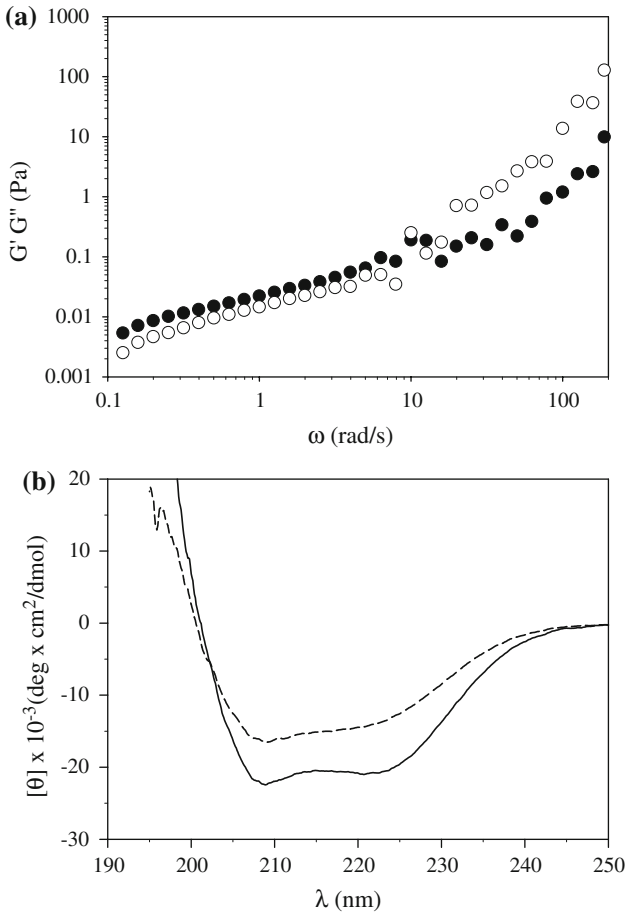

Fig. 5 **a** Elastic (G') (●) and viscous (G'') (◯) moduli as function of angular frequency ω for BSA sample (1 mM) in MES buffer at $T = 20$°C after 2 h of incubation at 58°C. **b** Far UV CD spectra of BSA samples (1 mM) in MES buffer at $T = 20$°C before (*continuous line*) and at the end of the incubation period

character with an elastic modulus, G', slightly larger than the viscous one, G'', in the frequency range 0.1–200 rad/s confirming that after the thermal treatment, the globular protein solution is already structured but it remains a weak gel (less than 10 Pa) up to 24 h (data not shown). We have also measured the viscoelastic response of the native protein solution before the thermal incubation (not shown). The obtained spectrum showed the typical behaviour expected for a protein solution with $G'' > G'$.

Changes in the native secondary structure of the BSA have also been probed by CD measurements performed at the beginning and at the end of the incubation time (Fig. 5b) in the far UV region (190–250 nm). The observed change confirms a decrease of the ratio of α-helix/β-sheet component (Woody 1996).

The evolution of the band component at 1,615 cm^{-1} and the scattered light intensity measured as a function of the incubation time (Fig. 6a) illustrate that changes at the level of secondary structure are related and simultaneous events to the growth of aggregates.

The results reported here, obtained in order to characterize the small aggregate origin under these experimental conditions, are in agreement with those obtained on BSA diluted in phosphate buffer (Militello et al. 2004), suggesting that the different solvent composition does not affect the aggregation process. Indeed, the present results show that at pD values far from the pI of the protein (~5), i.e. when the protein has a net charge, aggregation proceeds in an ordered way; the process is characterized by a partial unfolding simultaneous with the formation of β-aggregates of small dimensions, about 20 nm, originated by α-helix conversions into β-aggregated structures.

Before the addition of the metal ions FTIR and DLS measurements have been done in order to test if changes induced by the heating treatment were stable. Data (not shown) have confirmed that secondary and tertiary conformational changes and aggregate dimension remain unchanged after cooling of the solution.

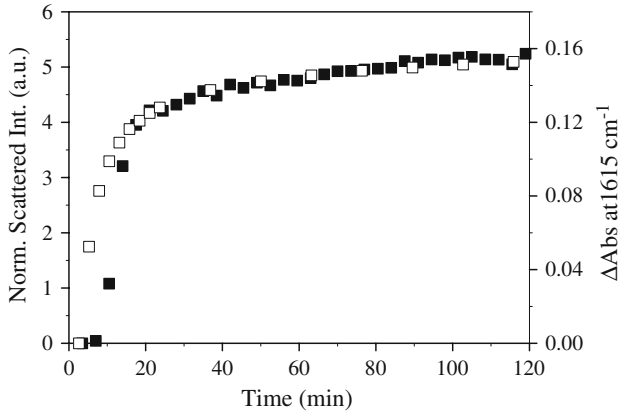

Fig. 6 Time evolution of the normalized scattering intensity, $(I(t)-I(0))/I(0)$, (■) and of the intensity of Amide I′ component assigned to β-aggregated structures (□) recorded during the incubation time at $T = 58$°C for BSA (1 mM) at pH = 7 $T = 20$°C

Gel characterization

The metal effects on the structural properties of the gels have been investigated by rheological measurements. In Fig. 7a and b, we report the elastic moduli obtained as a function of time for BSA samples at a frequency of 1 rad/s after addition of different concentrations of Cu^{2+} and Zn^{2+}, respectively. Except for the sample at the lowest metal concentration (1 mM Cu^{2+} or Zn^{2+}), all samples exhibit a marked solid-like character a few minutes after metal addition as evidenced by the large initial G' values. Figure 8 reports the G' values obtained from kinetic measurements at $t = 800$ min from the beginning for both Cu^{2+} and Zn^{2+}. Under these experimental conditions, a critical metal concentration has been identified. In fact, two different regimes are present at increasing metal concentration. Below 10 mM, the elastic modulus increases with rising metal concentration. On the contrary, above 10 mM we observe a decrease of the elastic parameter with increasing metal concentration.

In agreement with other authors (Doi 1993; Remondetto and Subirade 2003), these results can be explained assuming that the supramolecular arrangement changes as a function of the metal concentration: at pH values far from pI and at low ionic strength, the ions present in solution are not sufficient to shield the electrostatic charge present on the protein surface. In this case an ordered assembly occurs, whose growth takes place in a "preferential" linear direction. Under such condition, the network is formed by filamentous and fine structures. Gels obtained in this last case are transparent because of the small dimensions of the aggregates present in solution, and they exhibit a large elastic value (Tobitani and Ross-Murphy 1997). On the contrary, the addition of large ion amounts is capable of shielding the charge present on the surface of proteins,

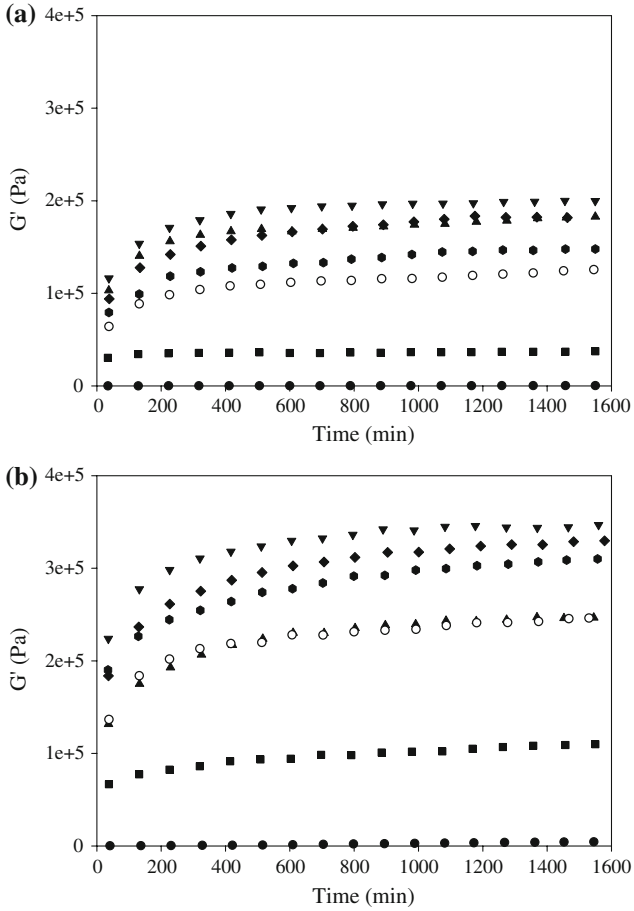

Fig. 7 Evolution of the storage modulus (G') in function of time for BSA 1 mM, pH = 7 at the frequency of 1 rad/s. All samples were kept 2 h at 58°C and then cooled at room temperature. Samples added of 1 mM (●), 5 mM (■), 8 mM (▲), 10 mM (▼), 15 mM (◆), 20 mM (⬢) and 30 mM (○) $CuCl_2$ (**a**) or $ZnCl_2$ (same symbols) (**b**)

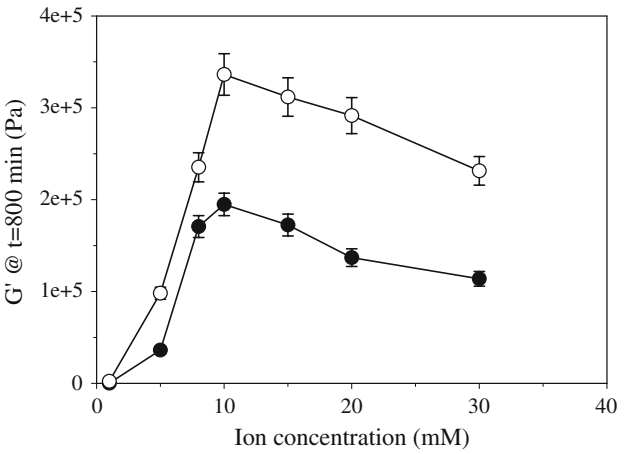

Fig. 8 G' values obtained from kinetics measurements at $t = 800$ min from the beginning of the kinetic at the frequency of 1 rad/s in function of Cu^{2+} (●) and Zn^{2+} (○) concentration

reducing the energy barrier preventing their approaching. When formed under these conditions, gels are made up by random and spherical aggregates connected in the so called "particulate gels". The network is coarse, opaque and brittle and characterized by a low elasticity (Tobitani and Ross-Murphy 1997). At intermediate metal/protein ratio, both filamentous and random structures are simultaneously present in the sample (Dickinson 1992; Doi 1993).

Under the present experimental conditions (1 mM BSA and pH 7.0), the critical metal concentration value,10 mM, remains unchanged in the presence of copper or zinc, suggesting that the cold-gelation process is governed by a charge effect. Further, these results are in agreement with data concerning investigations carried out on different protein cold-gels induced by different salts. Remondetto et al. (2002) and Remondetto and Subirade (2003) have investigated 6% (w/v) iron induced cold-gels of βLg having the same pI value as BSA. They found a decrease of the elastic modulus by changing the ion concentration from 10 mM to 40 mM. Furthermore, Marangoni et al. (2000), exploring the structure of Whey Protein Isolate (WPI) cold-gels induced by $CaCl_2$, have identified the maximum of elastic modulus as a function of salt concentration at 30 mM.

Further, Fig. 8 shows that, at a given metal concentration, the presence of Zn^{2+} enhances the elastic character of the network as indicated by the larger G' value. Data here presented are in agreement with results obtained by Haque and Aryana (2002) for the thermal gelation of BSA. In fact, they found that the addition of 5 mM $ZnSO_4$ to BSA solutions causes the formation of a more compact and clustered gel than that obtained in presence of $CuSO_4$. This behaviour could be explained assuming that metal ions play another important and direct role in the cold-gelation of proteins because of their ability to act as bridges between the negative charged groups present on two neighbouring protein molecules (Ball et al. 1998; Bryant and McClements 1998; Remondetto and Subirade 2003) and supposing that more sites are available on the protein surface for Zn^{2+} bridges rather than for Cu^{2+}. This could make the occurrence of links between different BSA molecules more frequent, accounting for the higher G' values observed in Zn^{2+} cases.

Conclusions

In the present work, the whole cold-gelation process of BSA in the presence of different concentrations of copper and zinc ions has been characterized. The first step of the experimental approach is focused on the characterization of the size and structure of particles present in solution via FTIR, DLS, CD and rheological measurements. These techniques have allowed us to obtain information on the secondary and tertiary structural changes occurring during the heating treatment and on the mean dimension of the protein assemblies. After 2 h of incubation at 58°C, we have observed the presence of small aggregates of about 20 nm in size, originating from the conversion of native α-helices into β-aggregates. The heated BSA solution showed a weak "solid-like" character, in agreement with the expected protein behaviour outlined by San Biagio et al. 1996 in the phase diagram of BSA solution. In the second step, we have investigated the viscoelastic properties of gels formed immediately after the addition of different amounts of the two metal ions, copper or zinc, in solution. It is the first time that BSA cold-gels have been induced by these metal ions. All samples exhibited a very high elastic character a few minutes after the metal addition. The elastic and viscous moduli strongly depend on metal concentration and two regimes can be distinguished below and above 10 mM. This behaviour supports the hypothesis that two effects play an important role in the network formation: the shielding action exerted by ions against the charges present on the protein surface and the "bridging" effect due to the ability of the ion in coordinating several oligomeric structures. Further, the hypothesis that on the protein surface more sites are available for Zn^{2+} rather than for Cu^{2+} bridges can explain the higher G' value obtained in the presence of Zinc.

Results here presented suggest that, by an appropriate choice of copper or zinc concentrations, it is feasible to obtain BSA cold-gels with the desired texture for industrial, food and pharmaceutical applications.

Acknowledgments This work was supported by a national project (PRIN2005) of the Italian Ministry of University Research. Partial financial support is also received from project "P.O.R. Regione Sicilia—Misura 3.15—Sottoazione C". We are indebted to Drs. D. Bulone and V. Vetri for useful discussions. We also wish to thank Mrs. F. Ferrante, D. Francofonte, G. Lapis, M. Lapis and G. Napoli for their very useful technical help.

References

Allain AF, Paquin P, Subirade M (1999) Relationships between conformation of β-lactoglobulin in solution and gel states as revealed by attenuated total reflection Fourier transform infrared spectroscopy. Biol Macromol 26:337–344. doi:10.1016/S0141-8130(99)00104-X

Alting AC, Hamer RJ, de Kruif CG, Visschers RW (2000) Formation of disulfide bonds in acid-induced gels of preheated whey protein isolate. J Agric Food Chem 48:5001–5007. doi:10.1021/jf000474h

Alting AC, Hamer RJ, de Kruif CG, Visschers RW (2003a) Cold-set protein gels; interactions, structure and rheology as a function of protein concentration. J Agric Food Chem 51:3150–3156. doi:10.1021/jf0209342

Alting AC, Hamer RJ, de Kruif CG, Paques M, Visschers RW (2003b) Hardness of cold set whey protein gels determined by

the amount of thiol groups rather than by the size of the aggregates. Food Hydrocoll 17:469–479. doi:10.1016/S0268-005X(03)00023-7

Alting AC, Weijers M, de Hoog EHA, van de Pijpekamo AM, Cohen Stuart MA, Hamer RJ, de Kruif CG, Visschers RW (2004) Acid-induced cold gelation of globular proteins: effects of protein aggregate characteristics and disulfide bonding on rheological properties. J Agric Food Chem 52:623–631. doi:10.1021/jf034753r

Bakker JM, Plützer C, Hünig I, Häber T, Compagnon I, von Helden G, Meijer G, Kleinermanns K (2005) Folding structures of isolated peptides as revealed by gas-phase mid-infrared spectroscopy. Chem Phys Chem 6:120. doi:10.1002/cphc.200400345

Ball W, Christodoulou J, Sadler PJ, Tucker A (1998) Multi-metal binding site of serum albumin. J Inorg Biochem 70:33–39. doi:10.1016/S0162-0134(98)00010-5

Barbut S, Foegeding EA (1993) Ca2+-induced gelation of pre-heated whey protein isolate. J Food Sci 58:867–871. doi:10.1111/j.1365-2621.1993.tb09379.x

Böhme U, Scheler U (2007) Effective charge of bovine serum albumin determined by electrophoresis and NMR. Chem Phys Lett 435:342–345. doi:10.1016/j.cplett.2006.12.068

Boye JI, Alli I, Ismail AA (1996) Interactions involved in the gelation of bovine serum albumin. J Agric Food Chem 44:996–1004. doi:10.1021/jf950529t

Berne BJ, Pecora R (1976) Dynamic light scattering. Wiley Interscience, New York (NY)

Bryant CM, McClements DJ (1998) Molecular basis of protein functionality with special consideration of cold-set gels derived from heat-denatured whey. Trends Food Sci Technol 9:143–151. doi:10.1016/S0924-2244(98)00031-4

Bryant CM, McClements DJ (2000) Influence of NaCl and CaCl2 on cold-set gelation of heat-denatured whey protein. J Food Sci 65:801–804. doi:10.1111/j.1365-2621.2000.tb13590.x

Byler DM, Susi H (1986) Examination of the secondary structure of proteins by deconvolved FTIR spectra. Biopolymers 25:469–487. doi:10.1002/bip.360250307

Cai S, Singh BR (1999) Identification of b-turn and random coil amide III infrared bands for secondary structure estimation of proteins. Biopolymers 80:7–20

Carter DC, Ho JX (1994) Structure of serum albumin. Adv Protein Chem 45:153–203. doi:10.1016/S0065-3233(08)60640-3

Dickinson E (1992) Introduction to food colloids. Oxford University Press, New York

Dobson CM (2004) Principles of protein folding, misfolding and aggregation. Semin Cell Dev Biol 15:3–16. doi:10.1016/j.semcdb.2003.12.008

Doi E (1993) Gels and gelling of globular proteins. Trends Food Sci Technol 1:1–5. doi:10.1016/S0924-2244(05)80003-2

Donato L, Garnier C, Novales B, Doublier JL (2005) Gelation of globular protein in presence of low methoxyl pectin: effect of Na+ and/or Ca2+ ions on rheology and microstructure of the systems. Food Hydrocoll 19:549–556. doi:10.1016/j.foodhyd.2004.10.019

Dong A, Huang P, Caughey WS (1990) Protein secondary structures in water from second-derivative Amide I infrared spectra. Biochemistry 29:3303–3308. doi:10.1021/bi00465a022

Fang Y, Dalgleish DG (1997) Conformation of β-lactoglobulin studied by FTIR: effect of pH, temperature, and adsorption to the oil–water interface. J Colloid Interface Sci 196:292–298. doi:10.1006/jcis.1997.5191

Fink AL (1998) Protein aggregation: folding aggregates, inclusion bodies and amyloid. Fold Des 30:R9–R23. doi:10.1016/S1359-0278(98)00002-9

Fogh-Andersen N, Bjerrum PJ, Siggard-Andersen O (1993) Ionic binding, net charge and Donnan effect of human serum albumin as a function of pH. Clin Chem 39:48–52

Gelamo EL, Tabak M (2000) Spectroscopic studies on the interaction of bovine (BSA) and human (HSA) serum albumins with ionic surfactants. Spectrochim Acta A Mol Biomol Spectrosc 56:2255–2271. doi:10.1016/S1386-1425(00)00313-9

Gelamo EL, Silva CHTP, Imasato H, Tabak M (2002) Interaction of bovine (BSA) and human (HSA) serum albumins with ionic surfactants: spectroscopy and modelling. Biochim Biophys Acta 1594:84–99

Gosal WS, Ross-Murphy SB (2000) Globular protein gelation. Curr Opin Colloid Interface Sci 5:188–194. doi:10.1016/S1359-0294(00)00057-1

Gosal WS, Clark AH, Ross-Murphy SB (2004a) Fibrillar β-lactoglobulin gels; part 1. Fibril formation and structure. Biomacromolecules 5:2408–2419. doi:10.1021/bm049659d

Gosal WS, Clark AH, Ross-Murphy SB (2004b) Fibrillar β-lactoglobulin gels; part 2. Dynamic mechanical characterization of heat-set system. Biomacromolecules 5:2420–2429. doi:10.1021/bm049660c

Haque ZZ, Aryana KJ (2002) Effect of copper, iron, zinc and magnesium ions on bovine serum albumin gelation. Food Sci Technol Res 8:1–3. doi:10.3136/fstr.8.1

Honda C, Kamizono H, Samejima T, Endo K (2000) Studies on thermal aggregation of bovine serum albumin as a drug carrier. Chem Pharm Bull (Tokyo) 48:464–466

Hongsprabhas P, Barbut S (1997a) Structure-forming processes in Ca^{2+}-induced whey protein isolate cold gelation. Int Dairy J 7:827–834. doi:10.1016/S0958-6946(98)00011-9

Hongsprabhas P, Barbut S (1997b) Effects of N-ethylmaleimide and $CaCl_2$ on cold gelation of whey protein isolate. Food Res Int 30:451–455. doi:10.1016/S0963-9969(97)00068-9

Hongsprabhas P, Barbut S (1997c) Ca^{2+}-induced cold gelation of whey protein isolate: effect of two stage gelation. Food Res Int 30:523–527. doi:10.1016/S0963-9969(98)00010-6

Hongsprabhas P, Barbut S, Marangoni AG (1999) The structure of cold-set whey protein isolate gels prepared with Ca^{++}. Lebenson Wiss Technol 32:196–202

Kavanagh GM, Clark AH, Ross-Murphy BS (2000) Heat-induced gelation of globular proteins: part 3. Molecular studies on low pH β-lactoglobulin gels. Int J Biol Macromol 28:41–50. doi:10.1016/S0141-8130(00)00144-6

Le Bon C, Nicolai T, Durand D (1999) Kinetics of aggregation and gelation of globular proteins after heat-induced denaturation. Macromolecules 32:6120–6127. doi:10.1021/ma9905775

Lefevre T, Subirade M (1999) Structural and interaction properties of β-lactoglobulin as studied by FTIR spectroscopy. Int J Food Sci Technol 34:419–428. doi:10.1046/j.1365-2621.1999.00311.x

Marangoni AG, Barbut S, McGauley SE, Marcone M, Narine SS (2000) On the structure of particulate gels—the case of salt-induced cold gelation of heat-denatured whey protein isolate. Food Hydrocoll 14:61–74. doi:10.1016/S0268-005X(99)00046-6

Militello V, Vetri V, Leone M (2003) Conformational changes involved in thermal aggregation processes of bovine serum albumin. Biophys Chem 105:133–141. doi:10.1016/S0301-4622(03)00153-4

Militello V, Casarino C, Emanuele A, Giostra A, Pullara F, Leone M (2004) Aggregation kinetics of bovine serum albumin studied by FTIR spectroscopy and light scattering. Biophys Chem 107:175–187. doi:10.1016/j.bpc.2003.09.004

Mulvihill DM, Kinsella JE (1987) Gelation characteristics of whey proteins and beta-lactoglobulin. Food Technol 41(9):102–111

Navarra G, Leone M, Militello V (2007) Thermal aggregation of β-lactoglobulin in presence of metal ions. Biophys Chem 161:52–61. doi:10.1016/j.bpc.2007.09.003

Pan W, Galkin O, Filobelo L, Nagel RL, Vekilov PG (2007) Metastable mesoscopic clusters in solutions of sickle-cell

hemoglobin. Biophys J 92:267–277. doi:10.1529/biophysj.106.094854

Pelton JT, Mec Lean LR (2000) Spectroscopic methods for analysis of protein secondary structure. Anal Biochem 277:167–176. doi:10.1006/abio.1999.4320

Provencher SW (1982) CONTIN: A general purpose constrained regularization program for inverting noisy linear algebraic and integral equations. Comput Phys Commun 27:229–242. doi:10.1016/0010-4655(82)90174-6

Qi XL, Holt C, McNulty D, Clarke DT, Brownlow S, Gareth R, Jones GR (1997) Effect of temperature on the secondary structure of β-lactoglobulin at pH 6.7, as determined by CD and IR spectroscopy: a test of the molten globule hypothesis. Biochem J 324:341–346

Remondetto GE, Paquin P, Subirade M (2002) Cold gelation of β-lactoglobulin in the presence of iron. J Food Sci 67:586–595. doi:10.1111/j.1365-2621.2002.tb10643.x

Remondetto GE, Subirade M (2003) Molecular mechanisms of Fe^{2+}-induced β-lactoglobulin cold gelation. Biopolymers 69:461–469. doi:10.1002/bip.10423

San Biagio PL, Bulone D, Emanuele A, Palma MU (1996) Self-assembly of biopolymeric structures below the threshold of random cross-link percolation. Biophys J 70:494–499

San Biagio PL, Martorana V, Emanuele A, Vaiana SM, Manno M, Bulone D, Palma Vittorelli MB, Palma MU (1999) Interacting processes in protein coagulation. Proteins 37:116–120. doi:10.1002/(SICI)1097-0134(19991001)37:1<116::AID-PROT11>3.0.CO;2-I

Tobitani A, Ross-Murphy SB (1997) Heat-induced gelation of globular proteins. 1. Model for the effects of time and temperature on the gelation time of BSA gels. Macromolecules 30:4845–4854. doi:10.1021/ma970112j

Veerman C, Sagie LMC, Heck J, van der Linden E (2003) Mesostructure of fibrillar bovine serum albumin gels. Int J Biol Macromol 31:139–146. doi:10.1016/S0141-8130(02)00074-0

Wang W (1999) Instability, stabilization and formulation of liquid protein pharmaceuticals. Int J Pharm 185:129–188. doi:10.1016/S0378-5173(99)00152-0

Woody RW (1996) Theory of circular dichroism in proteins. In: Fasman GD (ed) Circular dichroism and the conformational analysis of biomolecules. Plenum Press, New York, pp 25–68

Ziegler GR, Foegeding EA (1990) The gelation of proteins. Adv Food Nutr Res 34:203–298. doi:10.1016/S1043-4526(08)60008-X